Abdominal Radiology

Published online: 27 August 2018

Abdom Radiol (2019) 44:473–481
https://doi.org/10.1007/s00261-018-1742-6

Evaluation of the diagnostic performance of apparent diffusion coefficient (ADC) values on diffusion-weighted magnetic resonance imaging (DWI) in differentiating between benign and metastatic lymph nodes in cases of cholangiocarcinoma

Julaluck Promsorn,[1] Wannaporn Soontrapa,[1] Kulyada Somsap,[1] Nittaya Chamadol,[1] Panita Limpawattana,[2] and Mukesh Harisinghani[3]

[1]Department of Radiology, Faculty of Medicine, Khon Kaen University, Khon Kaen 40002, Thailand
[2]Department of Internal Medicine, Faculty of Medicine, Khon Kaen University, Khon Kaen 40002, Thailand
[3]Department of Radiology, Massachusetts General Hospital, Harvard Medical School, 55 Fruit Street, Boston, MA 02114, USA

Abstract

Introduction: Cholangiocarcinoma (CCA) is the primary tumor found in the bile duct and is associated with a high incidence of lymph node (LN) metastases and poor outcomes. The presence of metastatic lymph nodes, when shown by imaging, can influence patient treatment and prognosis. DWI is a promising, non-invasive imaging technique for differentiating between benign and malignant LNs. Many studies have shown that LN metastases have a lower apparent diffusion coefficient (ADC) value when compared to benign nodes.

Objective: To evaluate the performance of ADC values as a basis for diagnosis of LN metastasis in cholangiocarcinoma patients.

Materials and methods: This was a retrospective imaging study that evaluated histopathologically proven intraabdominal LNs in cholangiocarcinoma patients who underwent a 1.5T abdomen MRI with DWI between January 2012 and July 2016. The ADC values and short-axis diameters of the LNs were measured and compared using student's *t* test. Receiver operating characteristic (ROC) curves were used to determine the threshold.

Results: A total of 120 lymph nodes—85 benign and 35 metastatic—were included. The mean short-axis diameter of the benign LNs (8.34 mm) was significantly lesser than that of the malignant LNs (9.56 mm). Receiver operating characteristic curve analysis using a size criterion of 1 cm yielded a value of 0.63. A diagnostic size criterion of 1 cm for the short axis was applied and yielded an accuracy of 66%, sensitivity/specificity of 41%/75%, and positive/negative predictive value of 34%/80%. The mean ADC values of metastatic (1.31×10^{-3} mm^2/s) LNs were not significantly different from those of non-metastatic LNs (1.29×10^{-3} mm^2/s).

Conclusion: There was no difference in terms of ADC value between benign lymph nodes and those with metastatic cholangiocarcinoma. Isolated measurement of the ADC value does not contribute to a diagnosis of lymph node metastasis.

Key words: DWI—ADC measurement—Cholangiocarcinoma lymph node metastasis

Cholangiocarcinoma (CCA) is the primary tumor found in the bile duct epithelium in both intrahepatic and extrahepatic locations. It has a high incidence rate in northeast Thailand (115:100,000 in men and 50:100,000 in women) [1]. The liver fluke *Opisthorchis viverrini* (OV) is an important risk factor of cholangiocarcinoma in this endemic area [1]. *Opisthorchis viverrini* inhabits the biliary system for decades causing chronic inflammation of the bile ducts and periductal fibrosis (PDF), leading to the development of cholangiocarcinoma [2, 3]. Lymph

Correspondence to: Julaluck Promsorn; *email:* pjulaluck@kku.ac.th

node (LN) metastasis is found in up to 50–60% of all cholangiocarcinoma patients and is associated with poor outcomes and prognoses [4]. Radical resection with a negative surgical margin is the only potential curative treatment for CCA. Patients who undergo radical resection have a 5-year survival rate of less than 40% [5, 6], while the most patients who are left untreated have a median survival of only 6 months [7].

Preoperative staging of the tumor plays an important role in evaluating resectability. The AJCC Cancer Staging Manual 7th Edition classified lymph node metastases into two categories: (1) N1 (lymph node metastases along the cystic duct, common bile duct, hepatic artery, and portal vein), which are classified as resectable and (2) N2 (lymph node metastases along the periaortic, pericaval, superior mesenteric, and celiac artery), which are classified as unresectable [8]. In general, imaging criteria for metastatic lymph nodes are that the lymph nodes are larger than 10 mm in short-axis diameter, they exhibit central necrosis, and are hyper-enhanced compared to liver parenchyma in the porto-venous phase on CT imaging [9]. The sensitivities and specificities of CT, MRI, and FDG-PET in LN staging among CCA patients are modest [10–12]. A non-invasive technique that accurately assesses lymph node metastasis would be of great benefit to patients, since surgical lymph node dissection (which is regarded as the gold standard method for diagnosis of lymph node metastasis) increases the cost and time of diagnosis, as well as the risk of complications to the patient. A non-invasive test would lead to fewer post-treatment complications and lower costs [13].

Recently, many studies have sought to use DWI as a biomarker for tumor detection and characterization, as well as for evaluating the spread of tumors to lymph nodes [14–22]. Malignant LNs have lower apparent diffusion coefficient (ADC) values than benign lesions, which have lower cellularity, smaller nuclei, lower nucleus-to-cytoplasm ratios, and more extracellular space [23, 24]. A calculated ADC value below 1.25×10^{-3} mm^2/s has been shown to serve as a threshold in differentiating between benign and malignant LNs [25].

The objective of this study was to evaluate the performance of DWI in the diagnosis of LN metastasis in an area endemic for cholangiocarcinoma.

Materials and methods

Patients

This study was approved by an institutional review board. We retrospectively reviewed all cholangiocarcinoma-diagnosed patients who had pathologically evaluated intraabdominal lymph nodes and had undergone MRI examination of the upper abdomen (including cases in which the DWI technique was used) in a busy tertiary care cancer hospital during the period between January 2012 and July 2016.

We excluded cases in which patients had received previous surgical or non-surgical treatment, the quality of the DWI was inadequate, there was inadequate documentation of lymph nodes location, or there was a pathological result. The final study population consisted of 120 lymph nodes.

All the patients underwent surgery and local lymph node dissection. Histopathological confirmation was performed on all resected lymph nodes. The surgically resected lymph nodes were documented and anatomically labeled in a standard location pattern per the surgical gastric cancer lymph node station grid [26] by the surgeon, which allowed the pathologist and radiologist to correlate the pathologic and radiologic results. All the lymph nodes were classified as either metastatic or non-metastatic. In cases which there were multiple metastatic lymph nodes within the same station, only the largest was analyzed.

Image analysis

A gastrointestinal radiologist with 10 years' experience in abdominal MR imaging evaluated the images using a PACS workstation. Images were analyzed in random order. The reader was blind to all the patients' information, pathological results, and MRI reports.

Quantitative analysis was performed by measuring the apparent diffusion coefficients (ADCs) of each node on an independent work station with an ADC map covering as much of the lymph node as possible and on which regions of interest were manually marked. Three ADC measurements were conducted on each node. They were then averaged to get the final ADC value. The corresponding DWI and T2-weighted images were used to assist in identifying the lymph node. The necrotic areas within the lymph node which showed T2 shine-through on DWI and ADC maps were not included in the measurements.

The short-axis diameter of each lymph node underwent three measurements, of which the average was used to obtain the final short-axis diameter.

MRI protocol

Magnetic resonance imaging was performed using a 1.5-T system (Magnetom Aera, Siemens Medical Solutions, Erlangen, Germany) with 16-channel body phased array coils anterior and two spine clusters (three channels each) posterior.

A coronal T2-weighted half-Fourier single-shot turbo spin-echo (HASTE) sequence and an axial T2-weighted turbo spin-echo sequence, as well as an axial dynamic T1-weighted, three-dimensional spoiled gradient-recalled echo sequence [volumetric interpolated breath-hold

examination (VIBE) sequence with spectral fat saturation] following the intravenous administration of Gd-DTPA, were acquired.

Diffusion-weighted images were acquired using a single-shot echo-planar imaging sequence. Thus, the gradient factors (*b* values) were 0, 150, and 800 s/mm^2. The technical parameters were as follows: echo time, 65 ms; EPI factor, 125; echo spacing, 0.77 ms; receiver bandwidth, 1736 Hz/pixel; spectral fat saturation; field of view, 292 × 360 mm; matrix, 125 × 192; section thickness, 6 mm. Integrated parallel imaging techniques (iPAT) by means of generalized auto-calibrating partially parallel acquisitions (GRAPPA) with a two-fold acceleration factor were used to shorten the echo train length. Prospective acquisition correction (PACE) was implemented for respiratory triggering. Data were acquired during the end-expiratory phase. Diffusion-weighted imaging was performed before the administration of Gd-DTPA.

Statistical analysis

Demographic data were analyzed using descriptive statistics and are presented in terms of percentage, mean, and standard deviation.

Continuous variables of ADC values and the diameters of benign and malignant lymph nodes were compared using student's *t* test.

A receiver operating characteristic (ROC) curve was used to summarize the overall accuracy of DWI using ADC measurement in detecting metastatic lymph nodes. Then an optimal cut-off point was determined. The performance of the test was summarized by the sensitivity, specificity, positive predictive value (PPV), and negative predictive value (NPV). All data analyses were carried out using SPSS (version 19.0, SPSS Inc., Chicago, IL).

Sample size calculation

The sample size calculation was based on the objective of the study, which is to assess the performance of DWI using ADC measurement in detecting metastatic lymph nodes in patients with cholangiocarcinoma. An absolute precision formula was used to estimate the population mean. We determined that a sample size of at least 116 cases of intraabdominal lymph nodes would be suitable to conduct this study in clinical practice with a 20% disease rate and 20% estimation error.

Results

We reviewed 63 patients (39 males and 24 females) who underwent 1.5T abdomen MRIs with diffusion-weighted images. The mean age was 62.38 ± 8.28 years (range 37–80 years). A total of 120 lymph nodes (85 benign lymph nodes and 35 metastatic lymph nodes) were included in the study. The baseline characteristics of the study population and lymph node locations are shown in Table 1.

The mean short-axis diameters of benign and malignant lymph nodes were 8.34 (± 2.39) mm and 9.56 (± 3.12) mm, respectively. The benign lymph nodes appeared significantly shorter in diameter than the malignant lymph nodes with $P = 0.047$, as shown in Fig. 1. Receiver operating characteristic curve analysis also showed modest diagnostic characteristics. The area under the curve was 0.63, with $P = 0.026$, as shown in Fig. 2. The usual size criteria of 1 cm of short-axis diameter was applied and yielded a sensitivity/specificity of 41%/75%, positive/negative predictive value of 34%/80%, and 66% accuracy in differentiating between malignant and benign lymph nodes in our population. When the short axis cut-off point was dropped to 7.86 cm to differentiate between benign and malignant lymph nodes, it resulted in sensitivity of 51% and specificity of 37%, as shown in Fig. 3.

All of the lymph nodes appeared to have higher signal intensity on higher diffusion sensitizing gradient (*b* value) at 0 s/mm^2, 150 s/mm^2, and 800 s/mm^2 and consequently low signal intensity on ADC maps (Figs. 4, 5, 6).

The mean ADC values of metastatic and non-metastatic nodes on DWI were 1.31×10^{-3} mm^2/s and 1.29×10^{-3} mm^2/s, respectively, as shown in Fig. 7. However, we found no significant difference in the ADC values of benign and malignant lymph nodes (P value = 0.76).

Receiving operating characteristic analysis also found that the ADC values had no diagnostic characteristics that could aid in differentiation between metastatic and non-metastatic nodes ($P = 0.76$) with an area under the curve of 0.518, as shown in Fig. 8.

Discussion

The differentiation between benign and malignant lymph nodes is important for both staging and determining resectability in cases of cholangiocarcinoma. However,

Table 1. Demographic data of the study population

Patients (number)	63
Mean age (years ± SD)	62.38 (± 8.28) (range 37–80)
Sex	
Male	39
Female	24
Lymph nodes (number)	120
Location	
Hepatoduodenal ligament	52
Common hepatic artery	43
Posterior pancreatic head	10
Paraaortic	6
Cystic duct	5
Celiac	2
Left gastric artery	1
Superior mesenteric artery	1

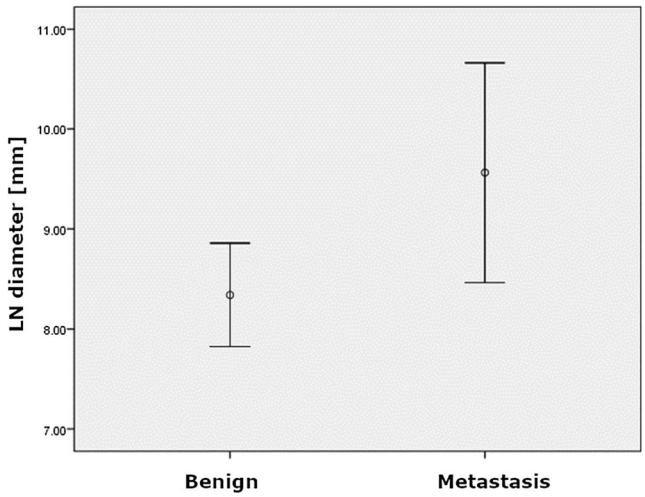

Fig. 1. Mean diameter of benign and malignant lymph nodes. The mean diameter of benign lymph nodes was significantly lesser than that of malignant lymph nodes ($P = 0.047$).

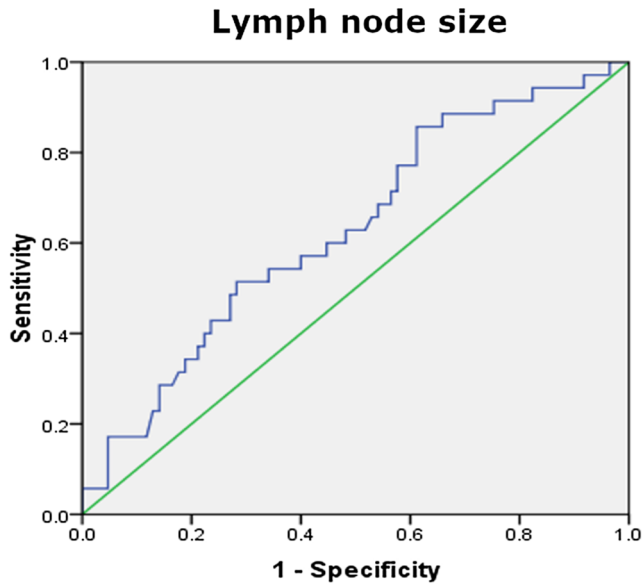

Fig. 2. ROC curve for differentiating between benign and malignant lymph nodes using short-axis diameter. The area under the ROC curve was 0.63 which has no diagnostic characteristics. $P = 0.026$.

published studies have shown that none of the established morphology criteria, including size, shape, or presence of necrosis, are very reliable for nodal characterization [25, 27, 28].

Recent studies have found metastatic lymph nodes to be significantly larger than non-metastatic nodes, but the clinical usefulness of LN size is still questionable [25, 27, 28]. The traditional size criterion for metastasis is a short-axis diameter of more than 10 mm [13, 25]. However, our study demonstrated that a lymph node size criterion of 10 mm resulted in limited diagnostic accuracy in terms of distinguishing between benign and metastatic lymph nodes (sensitivity/specificity = 34%/80%, positive/negative predictive value = 41%/25%, accuracy = 66%). Receiving operating characteristic curve analysis showed modest diagnostic characteristics with an AUC of 0.63 ($P = 0.026$), which suggested that LN size had moderate usefulness in predicting LN metastasis. Reducing the size threshold for characterizing nodes enhances sensitivity but does so at the expense of specificity. This was also shown in our study that dropping the short axis cut-off point to 7.86 cm to differentiate between benign and malignant lymph nodes yielded a sensitivity of 51% and specificity of 37%.

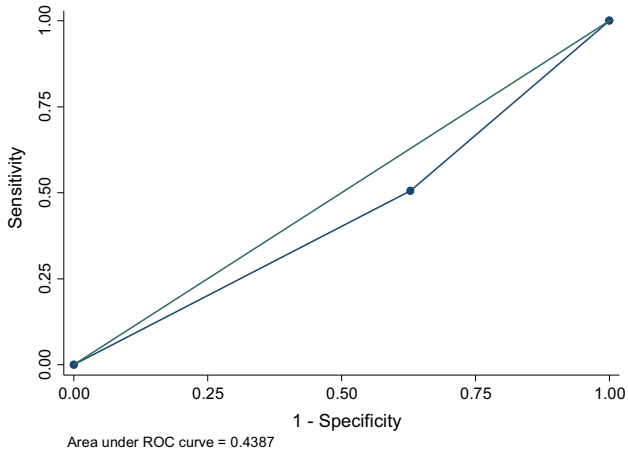

Fig. 3. ROC curve for differentiating between benign and malignant lymph nodes using a lymph node short axis cut-off point of 7.86, which yielded a sensitivity of 51% and specificity of 37%.

Ruys et al. [29] found similar results when they examined the efficacy of the size criterion for the detection of metastatic lymph nodes in patients with hilar cholangiocarcinoma. They took measurements from a section on a glass slide using a stereo microscope and found metastatic LNs to be significantly larger in short-axis and long-axis diameters than negative nodes. However, ROC analysis showed low AUC and there was no clear cut-off point.

Diffusion-weighted imaging is a non-invasive functional type of molecular imaging which does not require contrast medium administration and does not involve ionizing radiation [13, 30]. The ADC calculated from DWI images provides a quantitative parameter that reflects the effects of capillary perfusion and water diffusion related to the cellularity of the lesion. Malignant tumors exhibit high signal intensity in DW images with higher B values and lower ADC values than benign or normal tissue [27, 31]. Previous studies on various types of cancer have reported that DWI can be used to discriminate between metastatic nodes and benign lymph nodes with high degrees of accuracy, and many authors have reported significant differences in ADC between metastatic and normal lymph nodes.

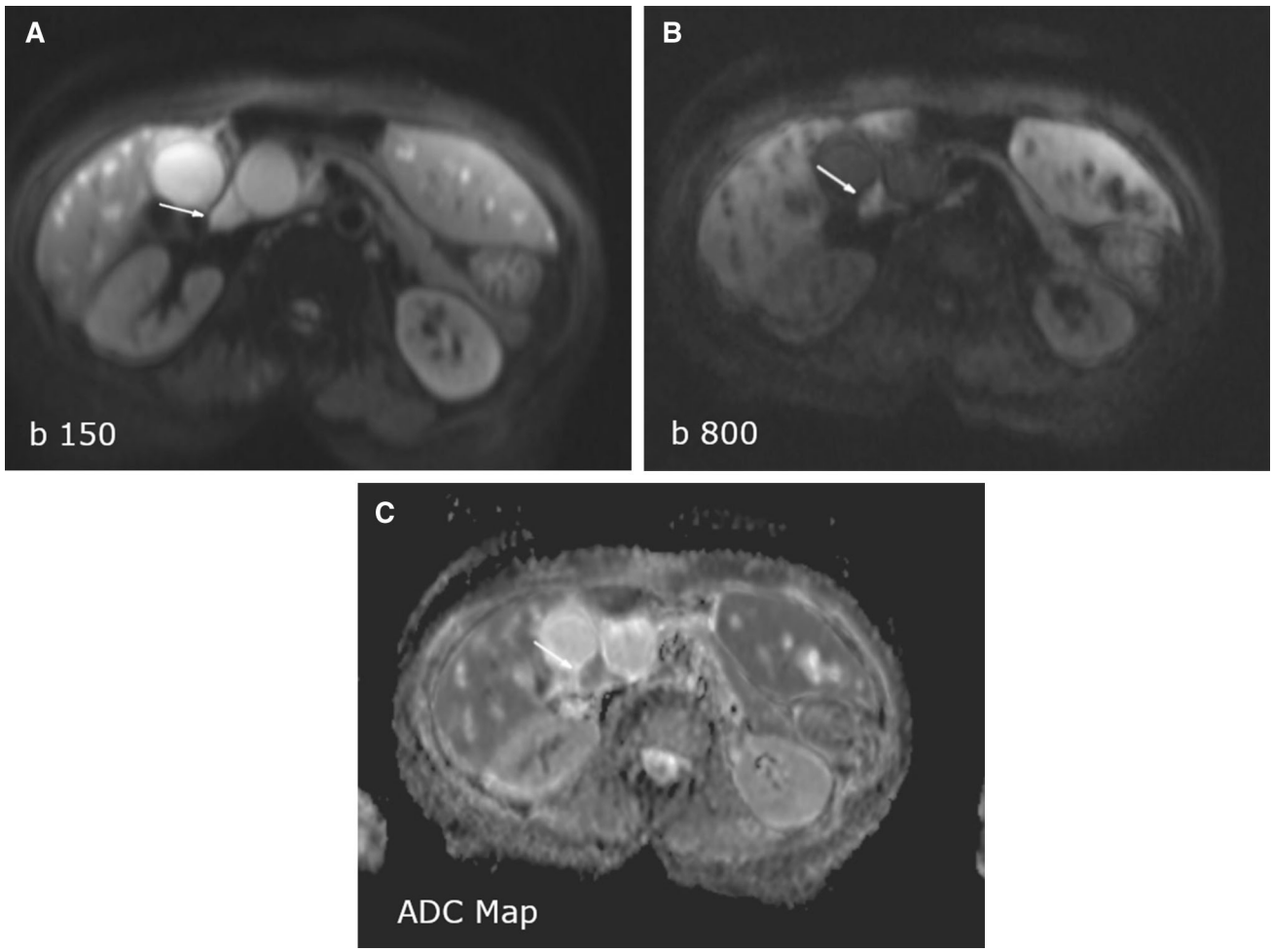

Fig. 4. A 68-year-old man with cholangiocarcinoma. DWI shows a lymph node at the hepatoduodenal ligament (arrow) with high signal intensity on low (**A**) and high *b* values (**B**) and relatively low signal intensity on the ADC map (**C**) with an ADC value of 1.43×10^{-3} mm^2/s. Histopathologic analysis found no malignancy.

Holzapfel et al. [25] studied the performance of DWI in diagnosing metastatic lymph nodes in cases of cholangiocarcinoma using an ADC value of 1.25×10^{-3} mm^2/s as the threshold with a sensitivity and specificity of 83.3%/92.8% and positive/negative predictive value of 66.7%/96.7%. The results of our study differed from theirs, which could be due to the small number of the metastatic lymph nodes in their study cohort or differences in MRI techniques (they used a different *b* value).

Our study reported similar results to those found in a study by Roy et al. [27], who evaluated 259 pelvic lymph nodes with 180 control and 79 metastatic lymph nodes and found no differences in signal intensity on DWI or ADC values between normal and metastatic nodes. This is also consistent with the results of a study by Nakai et al. [31], which examined pelvic lymph nodes in gynecologic malignancies using DWI and found that ADC values did not indicate differences between metastatic and non-metastatic nodes to a statistically significant extent.

However, Yasui et al. [32] reported that DWI had an accuracy of 74.8% in detecting lymph node metastasis based on a study of 46 colorectal cancer patients using a cut-off ADC value of 1.44×10^{-3} mm^2/s. Li et al. [28] studied the diagnostic value of diffusion-weighted MRI for differentiating between metastatic and non-metastatic retropharyngeal lymph nodes in 145 patients with nasopharyngeal carcinoma with a sensitivity of 95.7%, specificity of 95.1%, and accuracy of 96.5% using a minimal ADC value of $0.89x10^{-3}$ mm^2/sec as the threshold for differentiating between metastatic and non-metastatic lymph nodes.

Although many studies have proven the feasibility of ADC for metastatic lymph node detection in various organs by showing that metastatic lymph nodes have lower ADC values than benign lymph nodes, the cut-off ADC value in each type of cancer seems to vary greatly according to the organ of the primary tumor. There are some explanations for this variance such as MRI

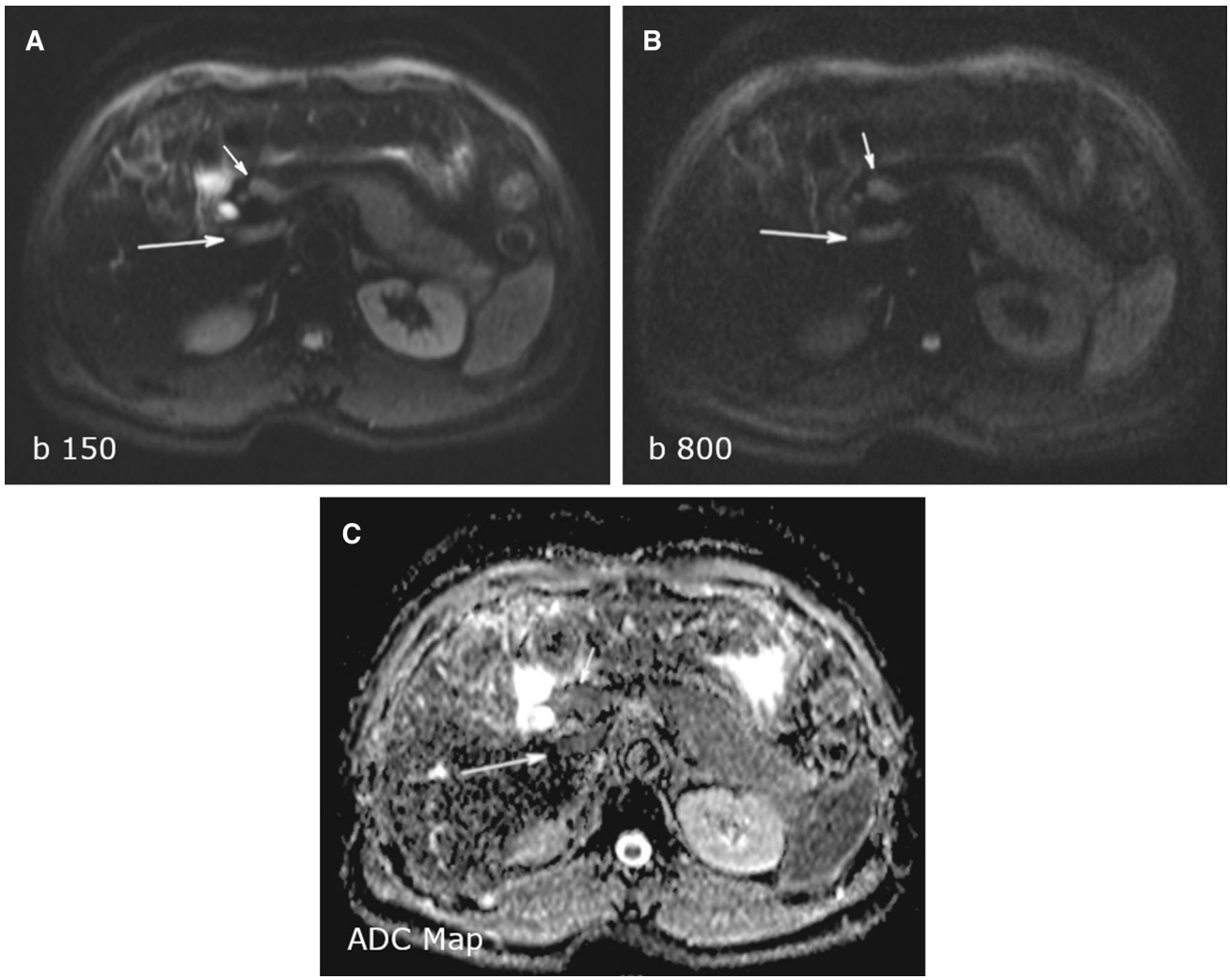

Fig. 5. A 53-year-old man with cholangiocarcinoma. DWI shows a lymph node at the hepatoduodenal ligament (long arrow) and hepatic artery (short arrow) with high signal intensity on low (**A**) and high *b* values (**B**) and relatively low signal intensity on the ADC map (**C**) with ADC values of 1.03×10^{-3} mm^2/s and 0.98×10^{-3} mm^2/s, respectively. Histopathologic analysis revealed lymph node metastasis of the hepatoduodenal lymph node and reactive hyperplasia of the hepatic artery lymph node. There was no significant difference in terms of morphology and signal intensity between the two lymph nodes.

parameters, magnetic field, location and area of the ROI, patient age, and body temperature [27].

There are several issues regarding the usefulness of ADC in the proper diagnosis of metastatic lymph nodes. Firstly, not all metastatic lymph nodes are entirely replaced by cancer cells; metastatic lymph nodes may have areas of carcinoma interspersed with normal tissue. Although ADC values may differ between cancerous and non-cancerous areas within a single node, the mean ADC value of a metastatic lymph node may not be significantly lower than that of a non-metastatic node. Secondly, necrosis is a factor that influences diffusion, and as the amount of necrosis in an affected node increases, so does the ADC value. Thus, in our study, we excluded visible necrotic lymph nodes. However, pathological analysis has shown that micronecrosis is common in metastatic lymph nodes, which may still influence the mean ADC value. In contrast, in benign abnormalities, such as lipomatosis, sinus histocytosis, and follicular hyperplasia, can also restrict diffusion due to microstructural tissue alteration. Inflammatory lymph nodes, inflammatory cell infiltration, reactive hyperplasia, and fibrous connective tissue proliferation can be seen, which also limit the diffusion of water molecules, resulting in a decrease in ADC value. ADC has limitations in terms of differentiating between inflammatory lymph nodes and metastatic lymph nodes because an ADC value only reflects tissue diffusivity and is not specific for cancer cells [13, 28, 31].

Many previous studies have suggested employing lymphotropic nanoparticle-enhanced MRI (LNMRI) using ultrasmall superparamagnetic iron oxide particles

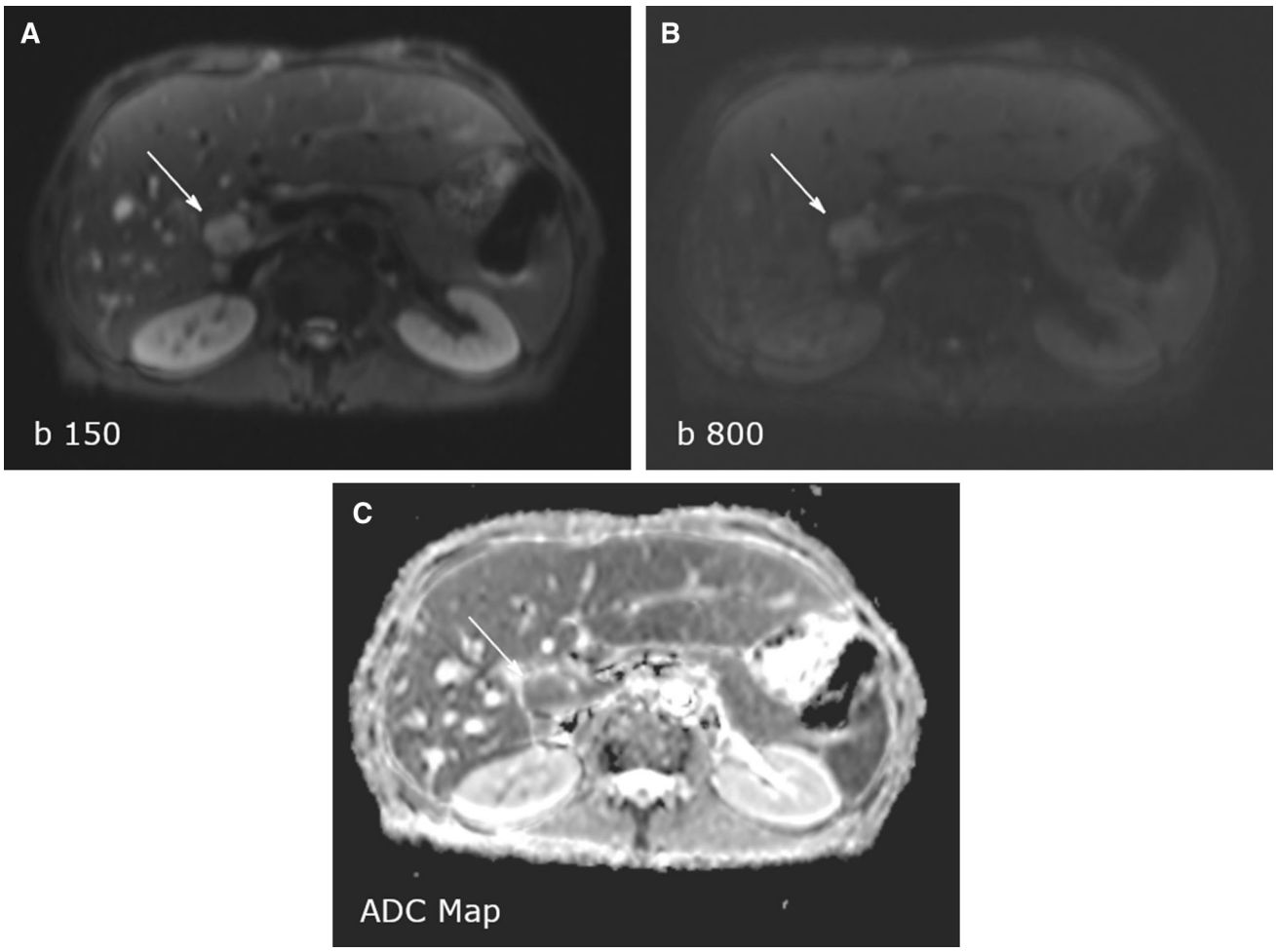

Fig. 6. A 61-year-old man with cholangiocarcinoma. DWI shows a lymph node at the hepatoduodenal ligament (arrow) with high signal intensity on low (**A**) and high *b* (**B**) values and relatively low signal intensity on the ADC map (**C**) with an ADC value of 1.05×10^{-3} mm^2/s. Histopathologic analysis suggested lymph node metastasis.

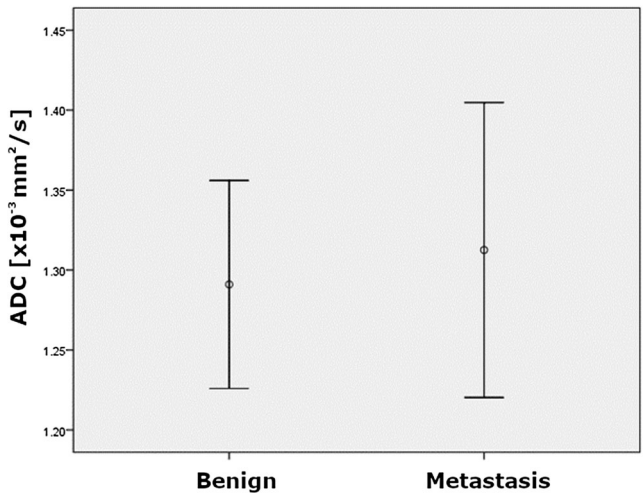

Fig. 7. Mean ADC values of benign and malignant lymph nodes. There was no statistically significant difference in the mean ADC values of benign and malignant lymph nodes ($P = 0.76$).

(USPIO), as ferumoxtran-10 is an emerging technique that is able to accurately differentiate between benign and metastatic lymph nodes in varying types of malignancy [33–44]. Recently, some studies have shown that LNMRI using the third-generation USPIOs, such as ferumoxytol (Feraheme; AMAG Pharmaceuticals), is also a non-invasive technique that improves lymph node staging in patients with pancreatic ductal adenocarcinoma with a sensitivity of 76.5% and specificity of 98.4%, which are higher than those of conventional imaging (CT, MRI, and PET/CT). It also has been shown to exhibit a high potential to outline primary tumors [45, 46]. However, this particle is not universally available.

Our study showed that DWI cannot be used to differentiate between metastatic and benign or reactive lymph nodes in cholangiocarcinoma patients. However, DWI is useful in detecting lymph nodes in these cases, especially N2 lymph nodes, which indicate non-surgical candidates. Laparoscopic lymph node biopsy with final pathology reports of these cases could reduce the number

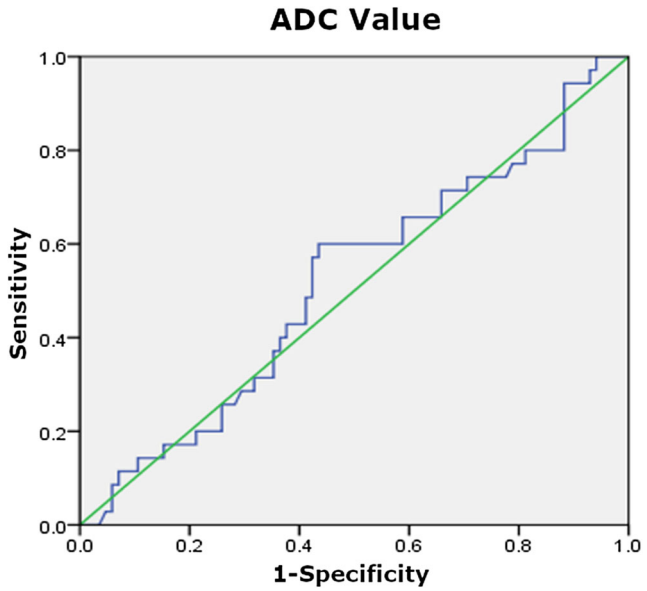

Fig. 8. ROC curve for differentiating between benign and malignant lymph node using ADC values. The area under the ROC curve was 0.518.

of unnecessary open hepatectomies that are performed and lead to better patient outcomes.

This study had several limitations. First, delineation of tiny structures like lymph nodes is challenging and has a high probability of succumbing to the partial volume effect, leading to inconsistent results, mainly in subcentimeter nodes. Second, although all of the lymph node assessments were confirmed by the pathological results, the pathological information did not mention whether the metastasis was microscopic or involved in the entire node. Third, the sizes and ADC values of lymph nodes were measured by only one gastrointestinal radiologist with 10 years' experience who specialized in abdominal MR imaging, which may have introduced some bias. However, since ADC is a quantitative measure, we believe there would be minimal change had there been more radiologists involved.

Conclusion

We found no difference in the ADC values between benign and metastatic lymph nodes in cases of cholangiocarcinoma. An isolated measurement of mean ADC does not contribute to a diagnosis of lymph node metastasis. However, benign lymph nodes are significantly smaller than malignant nodes, which showed mild diagnostic characteristics allowing for differentiation between these two conditions.

Acknowledgements We would like to acknowledge Dylan Southard (Research Affairs, Faculty of Medicine, Khon Kaen University, Thailand) for editing the manuscript.

Compliance with ethical standards

Funding This study was funded by Faculty of Medicine Khon Kaen University, Thailand (Grant Number IN60110).

Conflict of interest The authors declare that they have no conflict of interest.

Ethics approval All procedures performed in studies involving human participants were performed in accordance with the ethical standards of the institutional and/or national research committee and with the 1964 Helsinki declaration and its later amendments or comparable ethical standards.

Informed consent For this type of retrospective study, formal consent is not required.

References

1. Chamadol N, Pairojkul C, Khuntikeo N, et al. (2014) Histological confirmation of periductal fibrosis from ultrasound diagnosis in cholangiocarcinoma patients. J Hepatobiliary Pancreat Sci 21(5):316–322
2. Chamadol N (2014) *Imaging of Cholangiocarcinoma Khon Kaen*, 1st edn. Khon Kaen: Radiology Department, Faculty of Medicine, KKU
3. Kaewpitoon N, Kaewpitoon SJ, Pengsaa P, Sripa B (2008) *Opisthorchis viverrini*: the carcinogenic human liver fluke. World J Gastroenterol 14(5):666–674
4. Murakami Y, Uemura K, Hayashidani Y, et al. (2007) Pancreatoduodenectomy for distal cholangiocarcinoma: prognostic impact of lymph node metastasis. World J Surg 31(2):337–344
5. Unno M, Katayose Y, Rikiyama T, et al. (2010) Major hepatectomy for perihilar cholangiocarcinoma. J Hepatobiliary Pancreat Sci 17(4):463–469
6. Young AL, Prasad KR, Toogood GJ, Lodge JP (2010) Surgical treatment of hilar cholangiocarcinoma in a new era: comparison among leading Eastern and Western centers. Leeds J Hepatobiliary Pancreat Sci 17(4):497–504
7. Lau SH, Lau WY (2012) Current therapy of hilar cholangiocarcinoma. Hepatobiliary Pancreat Dis Int 11(1):12–17
8. Edge SB, Byrd DR, Compton CC, et al. (2010) Perihilar bile ducts. In: Amin MB, et al. (eds) *AJCC cancer staging handbook*, 7th edn. Chicago, IL: Springer, p 718
9. Lee HY, Kim SH, Lee JM, et al. (2006) Preoperative assessment of resectability of hepatic hilar cholangiocarcinoma: combined CT and cholangiography with revised criteria. Radiology 239(1):113–121
10. Roche CJ, Hughes ML, Garvey CJ, et al. (2003) CT and pathologic assessment of prospective nodal staging in patients with ductal adenocarcinoma of the head of the pancreas. AJR Am J Roentgenol 180(2):475–480
11. Kluge R, Schmidt F, Caca K, et al. (2001) Positron emission tomography with [(18)F]fluoro-2-deoxy-D-glucose for diagnosis and staging of bile duct cancer. Hepatology 33(5):1029–1035
12. Hänninen EL, Pech M, Jonas S, et al. (2005) Magnetic resonance imaging including magnetic resonance cholangiopancreatography for tumor localization and therapy planning in malignant hilar obstructions. Acta Radiol 46(5):462–470
13. Wang J, Liao Q, Zhang Y, et al. (2012) Differential diagnosis of axillary inflammatory and metastatic lymph nodes in rabbit models by using diffusion-weighted imaging: compared with conventional magnetic resonance imaging. Korean J Radiol 13(4):458–466
14. Qayyum A (2009) Diffusion-weighted imaging in the abdomen and pelvis: concepts and applications. Radiographics 29(6):1797–1810
15. Shinya S, Sasaki T, Nakagawa Y, et al. (2007) The usefulness of diffusion-weighted imaging (DWI) for the detection of gastric cancer. Hepatogastroenterology 54(77):1378–1381
16. Xue HD, Li S, Sun HY, Jin ZY, Sun F (2008) Experimental study of inflammatory and metastatic lymph nodes with diffusion weighted imaging on animal model: comparison with conventional methods. Chin Med Sci J 23(3):166–171

17. Mir N, Sohaib SA, Collins D, Koh DM (2010) Fusion of high b-value diffusion-weighted and T2-weighted MR images improves identification of lymph nodes in the pelvis. J Med Imaging Radiat Oncol 54(4):358–364
18. Lin C, Luciani A, Itti E, et al. (2010) Whole-body diffusion-weighted magnetic resonance imaging with apparent diffusion coefficient mapping for staging patients with diffuse large B-cell lymphoma. Eur Radiol 20(8):2027–2038
19. Eiber M, Beer AJ, Holzapfel K, et al. (2010) Preliminary results for characterization of pelvic lymph nodes in patients with prostate cancer by diffusion-weighted MR-imaging. Invest Radiol 45(1):15–23
20. Chen YB, Liao J, Xie R, Chen GL, Chen G (2011) Discrimination of metastatic from hyperplastic pelvic lymph nodes in patients with cervical cancer by diffusion-weighted magnetic resonance imaging. Abdom Imaging 36(1):102–109
21. Klerkx WM, Mali WM, Peter Heintz A, et al. (2011) Observer variation of magnetic resonance imaging and diffusion weighted imaging in pelvic lymph node detection. Eur J Radiol 78(1):71–74
22. Vallini V, Ortori S, Boraschi P, et al. (2015) Staging of pelvic lymph nodes in patients with prostate cancer: usefulness of multiple b value SE-EPI diffusion-weighted imaging on a 3.0T MR system. Eur J Radiol Open 3:16–21
23. Wang J, Takashima S, Takayama F, et al. (2001) Head and neck lesions: characterization with diffusion-weighted echo-planar MR imaging. Radiology 220(3):621–630
24. Le Bihan D, Breton E, Lallemand D, et al. (1986) MR imaging of intravoxel incoherent motions: application to diffusion and perfusion in neurologic disorders. Radiology 161(2):401–407
25. Holzapfel K, Gaa J, Schubert EC, et al. (2016) Value of diffusion-weighted MR imaging in the diagnosis of lymph node metastases in patients with cholangiocarcinoma. Abdom Radiol (NY) 41(10):1937–1941
26. Kim HJ, Karpeh MS, Brennan MF (2001) Standardization of the extent of lymphadenectomy for gastric cancer: impact on survival. Adv Surg 35:203–223
27. Roy C, Bierry G, Matau A, Bazille G, Pasquali R (2010) Value of diffusion-weighted imaging to detect small malignant pelvic lymph nodes at 3 T. Eur Radiol 20(8):1803–1811
28. Li H, Liu X-W, Geng Z-J, Wang D-L, Xie C-M (2015) Diffusion-weighted imaging to differentiate metastatic from non-metastatic retropharyngeal lymph nodes in nasopharyngeal carcinoma. Dentomaxillofac Radiol 44(3):20140126
29. Ruys AT, Ten Kate FJ, Busch OR, et al. (2011) Metastatic lymph nodes in hilar cholangiocarcinoma: does size matter? HPB (Oxford) 13(12):881–886
30. Padhani AR, Liu G, Koh DM, et al. (2009) Diffusion-weighted magnetic resonance imaging as a cancer biomarker: consensus and recommendations. Neoplasia 11(2):102–125
31. Nakai G, Matsuki M, Inada Y, et al. (2008) Detection and evaluation of pelvic lymph nodes in patients with gynecologic malignancies using body diffusion-weighted magnetic resonance imaging. J Comput Assist Tomogr 32(5):764–768
32. Yasui O, Sato M, Kamada A (2009) Diffusion-weighted imaging in the detection of lymph node metastasis in colorectal cancer. Tohoku J Exp Med 218(3):177–183
33. Anzai Y, Piccoli CW, Outwater EK, et al. (2003) Evaluation of neck and body metastases to nodes with ferumoxtran 10-enhanced MR imaging: phase III safety and efficacy study. Radiology 228(3):777–788
34. Anzai Y, Blackwell KE, Hirschowitz SL, et al. (1994) Initial clinical experience with dextran-coated superparamagnetic iron oxide for detection of lymph node metastases in patients with head and neck cancer. Radiology 192(3):709–715
35. Hoffman HT, Quets J, Toshiaki T, et al. (2000) Functional magnetic resonance imaging using iron oxide particles in characterizing head and neck adenopathy. Laryngoscope 110(9):1425–1430
36. Sigal R, Vogl T, Casselman J, et al. (2001) Lymph node metastases from head and neck squamous cell carcinoma: MR imaging with ultrasmall superparamagnetic iron oxide particles (Sinerem MR)—results of a phase-III multicenter clinical trial. Eur Radiol 12(5):1104–1113
37. Mack MG, Balzer JO, Straub R, Eichler K, Vogl TJ (2002) Superparamagnetic iron oxide—enhanced MR imaging of head and neck lymph nodes. Radiology 222(1):239–244
38. Harisinghani MG, Barentsz J, Hahn PF, et al. (2003) Noninvasive detection of clinically occult lymph–node metastases in prostate cancer. N Engl J Med 348:2491–2499
39. Deserno WM, Harisinghani MG, Taupitz M (2004) Urinary bladder cancer: preoperative nodal staging with ferumoxtran-10—enhanced MR imaging. Radiology 233(2):449–456
40. Stets C, Brandt S, Wallis F, et al. (2002) Axillary lymph node metastases: a statistical analysis of various parameters in MRI with USPIO. J Magn Reson Imaging 16(1):60–68
41. Michel SC, Keller TM, Frohlich JM, et al. (2002) Preoperative breast cancer staging: MR imaging of the axilla with ultrasmall superparamagnetic iron oxide enhancement. Radiology 225(2):527–536
42. Pannu HK, Wang KP, Borman TL, Bluemke DA (2000) MR imaging of mediastinal lymph nodes: evaluation using a superparamagnetic contrast agent. J Magn Reson Imaging 12(6):899–904
43. Nguyen BC, Stanford W, Thompson BH, et al. (1999) Multicenter clinical trial of ultrasmall superparamagnetic iron oxide in the evaluation of mediastinal lymph nodes in patients with primary lung carcinoma. J Magn Reson Imaging 10(3):468–473
44. Keller TM, Michel SC, Frohlich J, et al. (2004) USPIO-enhanced MRI for preoperative staging of gynecological pelvic tumors: preliminary results. Eur Radiol 14(6):937–944
45. Harisinghani MG, Ross RW, Guimaraes AR, Weissleder R (2007) Utility of a new bolus-injectable nanoparticle for clinical cancer staging. Neoplasia 9(12):1160–1165
46. McDermott S, Thayer SP, Castillo CF, et al. (2013) Accurate prediction of nodal status in preoperative patients with pancreatic ductal adenocarcinoma using next-gen nanoparticle. Transl Oncol 6(6):670–675